A comparison of turbulence models for the computation of a detached flow around a square cylinder

Maliska, C. R.[1], Paladino, E.E.[1], Saltara, F.[2], Contessi, B. A.[2]

Ataides, R[2] and Girardi Silva, V.[2]

[1] *CFD Lab-SINMEC, Federal University of Santa Catarina, Florianópolis, SC, Brazil*

[2]*ESSS-Engineering Simulation and Scientific Software, Florianópolis, SC, Brazil*

email: *maliska@sinmec.ufsc.br*

ABSTRACT

This paper presents a comparison of Large Eddy Simulation - LES and Scale Adaptative Simulation - SAS versus k-ω SST model, based on U-RANS approach, for the unsteady flow around a square cylinder. Although Large and Detached Eddy Simulation approaches have become more and more common for external flow problems with detached regions, depending on Reynolds number, the meshes and time steps needed to satisfy LES requirements are unpractical for industrial applications which require, for instance, parametrical studies or geometry optimization involving a huge set of runs. With this in mind, the main objective of this study is to verify the efficiency of the SAS model and also compare with the traditional less CPU demanding models based on URANS, SST, and the LES Dynamic model from Lilly [1]. Results from all models have been compared to experimental results provided by the organization [2] of the Challenging Problem of the 2012 CFD Society of Canada Annual Conference.

1. INTRODUCTION

Numerical simulation of external open flow problems with detached regions has represented a challenging issue for engineers and numerical analysts over the last three decades. The main shortcoming has been the lack of adequate turbulence models able to deal with large turbulent fluctuations within the detached regions. Traditional eddy viscosity or, even Reynolds Stress models, based on Reynolds Averaged Navier-Stokes (RANS) equations, are known to be limited for predicting flows that are strongly influenced by vortex-shedding. In those flows, as pointed out by Lardeau & Leschziner [3], the time scale of the largest turbulent eddies is dictated by the period of vortex-shedding. The need to properly capture the periodic flow requires a time step much smaller than the shedding period, what means that the time steps required are smaller than the time scale of the largest turbulent eddies. This fact is in contradiction with the theoretical assumptions related to RANS calculations. A solution for this problem is the usage of Large Eddy Simulation (LES) models in which the equations are not averaged but filtrated, calculating the flow structures of the larger turbulent eddies and modeling only the smaller incoherent ones, which, *a priori*, does not depend on the problem geometry. It is clear that this approach is intrinsically transient and fine meshes are required in order to ensure that all large structures, i.e. those which depend on geometry, are captured by the numerical solution.

Rodi ([4]) was among the first to point out that URANS simulations of the flow around bluff bodies produce inferior results when compared to LES simulations. In general, the shedding motion is under-predicted in URANS simulations. The k-ε model is known for being over-diffusive, in part due to the super-production of kinetic energy in stagnation points, a characteristic that, according to Craft ([6]) can be attributed to the Boussinesq assumption used to describe the Reynolds stresses.

Spalart ([5]) noted that the limitations of URANS simulations are particularly felt when 3D simulations of typical 2D geometries are performed. Results from Shur et al. ([7]) indicate that URANS simulations of the

flow around a circular cylinder clearly suppress the wake three-dimensionality, which means that drag and RMS lift coefficients are in general over-predicted.

On the other side, industrial applications require simulations with less demanding CPU time and usually involve several runs, for instance, for geometrical optimization. In this context, the usage of RANS approach has been mandatory. Among the several RANS models available in most commercial software the k-ω SST ([8]) is known to be able to deal with flows with adverse pressure gradient and detached regions, and this the model used in this work as reference for RANS approach. The comparison proposed in this paper intends to determine how transient RANS models (also called URANS), particularly k-ω SST model, are able to compute the flow in these type of problems, at least on mean parameters, as average velocities and aerodynamic forces.

One limitation of the LES approach for open flow problems is it inability to adequately compute the flow in boundary layer regions. In fact, this limitation arises not from the model itself, but from the relationship between the turbulent scales and smallest grid size. In detached region, largest turbulent scales are considered to be of order of main geometry scale, as a diameter or wing cord length. On the other side, within the boundary layer,the largest turbulent scales are of order of the boundary layer thickness. Then, the minimum mesh size required to capture turbulent structures which satisfy LES criteria could be impracticable within the boundary layers. A solution for this problem is introduced by the Scale Adaptive Simulation Models (SAS), which basically uses a RANS approach within non-detached region and LES in detached ones. Here, the Menter & Egorov ([9]) SST-SAS model is used and compared with LES Dynamic and k-ω SST models.

2. PROBLEM DESCRIPTION

The problem consists in the flow computation over a finite square cylinder with the side dimension d (d = 12.7 mm) and height h ($h = 4d$ = 50.4 mm). The flow around the obstacle has a free stream velocity of 15 m/s with a turbulence intensity of approximately 0.8%. Reynolds Number based on the side size (d) and free stream velocity (U_∞) is 11000.
The obstacle is mounted vertically in an open-section wind tunnel (zero streamwise pressure gradient) at a distance of 4h from the leading edge of the plate. Figure 1 schematically shows the obstacle, the dimensions involved in the problem. The lines where velocity and turbulent stresses will be compared against experimental results are also shown in the figure. The computational wind tunnel has 12d of height, 13d of width, 200 mm (*15.7d*) from the obstacle center to the inlet and 20d from the obstacle back face to the outlet.

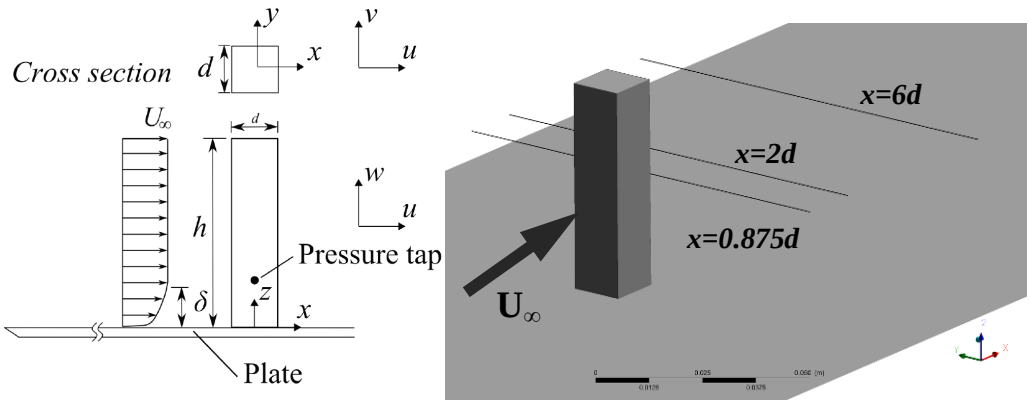

Figure 1 - Problem overview. Lines where profiles were compared are also shown.

3. COMPUTATIONAL MODEL

3.1 Governing Equations

The flow is considered to be incompressible, isothermal, and the governing equation are the mass and momentum conservation in their differential form.

Depending on the approach adopted for the turbulence calculation the momentum equation could be **averaged** after the application of Reynolds decomposition on velocity and pressure fields, for the case of RANS approach, or **filtered**, in the case of large or detached eddy simulation approaches. Application of Reynolds decomposition and averaging on the momentum equation, according to Pope ([10]), and considering an eddy viscosity based model, for the turbulent stress tensor, leads to,

$$\frac{\partial}{\partial t}(\rho\mathbf{U}) + \nabla\cdot(\rho\mathbf{U}\mathbf{U}) = -\nabla\left(P + \frac{2}{3}\rho k\right) + \nabla\cdot\left(\mu_{eff}\left(\nabla\mathbf{U} + \nabla\mathbf{U}^T\right)\right) + \mathbf{f} \quad (1)$$

where $\mu_{eff} = \mu + \mu_T$ is the effective viscosity and k is the turbulent kinetic energy. This variable and the turbulent viscosity, μ_T, are calculated through the k-ω SST model. Here, the variables in capital letters represent averages of instantaneous variables (in lowercase).

On the other side, in models intended to be able to capture large transient turbulent structures, the momentum equations are not averaged, but filtered (see, for instance, Layton ([11])) giving,

$$\frac{\partial}{\partial t}(\rho\mathbf{U}) + \nabla\cdot(\rho\mathbf{U}\mathbf{U}) = -\nabla P + \nabla\cdot\left(\mu_{eff}\left(\nabla\mathbf{U} + \nabla\mathbf{U}^T\right)\right) + \mathbf{f} + \nabla\cdot\boldsymbol{\tau} \quad (2)$$

where, introducing a sub-grid turbulent viscosity, one has

$$\boldsymbol{\tau} = \rho\overline{\mathbf{u}\mathbf{u}} - \rho\mathbf{U}\mathbf{U} = \mu_{SGS}\left(\nabla\mathbf{U} + \nabla\mathbf{U}^T\right) - \bar{\bar{\mathbf{I}}}\left(\tau_{ii}/3\right) \quad (3)$$

The sub-grid turbulent viscosity, μ_{SGS}, takes into account the contribution of the turbulent eddies, whose scales are smaller than the mesh size (and therefore not calculated), to the turbulent diffusion.

The SAS approach consists essentially in a URANS model, in this case k-ω SST, in which the von Karman length scale is introduced into the turbulence equations, allowing this model to dynamically adjust to resolved structures. This results in a LES-like behavior in the detached regions and RANS prediction in the boundary layer regions.

3.2 Turbulence models

In the URANS approach, all scales of the turbulent motion are modeled. In eddy-viscosity models like the k-ω SST model, the Boussinesq assumption is used to represent the Reynolds stresses, as

$$-\rho\overline{u_i' u_j'} = -\frac{2}{3}\rho\delta_{ij}k + 2\mu_t S_{ij} \quad (4)$$

Failure in simulating bluff-body flows would be due to the closeness of the time scale of vortex shedding and the time scale of the large turbulent eddies, and from the Boussinesq assumption. As pointed out by Craft ([6]) the linear relation between the Reynolds stresses and the deformation rate results in an over-prediction of the turbulence production near stagnation points. The excess of produced kinetic energy is convected to the wake, leading to higher levels of eddy viscosity that dissipate the turbulent structures.

For those reasons, in general LES or hybrid RANS-LES approaches are favored for the simulation of bluff-body flows. Through the spatial filtering operation performed in LES the large scales of the flow are directly solved, and since the large eddies are responsible for the majority of the turbulent kinetic energy spectrum of the flow, the smaller eddies can be modeled through very simple approaches like the Smagorinsky model, from Smagorinsky ([12]). In this model, the sub-grid stresses are modeled by,

$$\tau_{ij} = \overline{u_i u_j} - \overline{u_i}\,\overline{u_j} = (C_s\Delta)^2\sqrt{2S_{ij}S_{ij}} \quad (5)$$

In this last equation, Δ is the LES filter width that separates the resolved from the modeled scales, and it is related to the mesh spacing. In this work, Δ was taken as the cubic root of the cell volume. The Smagorinsky constant C_s is often considered in the range 0.1-0.25. In the present work the Dynamic Smagorinsky-Lilly model was employed and C_s was not taken as a constant, but dynamically evaluated for each cell during the time-stepping procedure following a method proposed by Germano et al. ([13]).

The LES approach has some major shortcomings. One is the need for some type of wall modeling that avoids the full solution of the boundary layer through the subgrid model, which would be prohibitively expensive in terms of computational cost, once the turbulent scales become smaller when the wall is approached. Other is the need for an almost isotropic mesh, with cells having almost the same dimensions in all directions, in order that the calculation of the mesh length scale through the cubic root of the cell volume is not hampered by the existence of high aspect-ratio cells. Scale-Adaptative Simulation (SAS) is a hybrid RANS-LES technique that addresses the issues related to LES through the utilization of a RANS k-ω SST model as a base model. The transport equation for the specific dissipation of turbulent kinetic energy (ω) is modified in relation to the RANS model through the addiction of a source term related to the Von Karman length scale L_{vk},

$$L_{vk} = \kappa \sqrt{2S_{ij}S_{ij}} \Bigg/ \sqrt{\sum_i \left(\frac{\partial^2 u_i}{\partial x_j \partial x_j} \right)^2} \tag{6}$$

In the last equation κ is the Von Karman constant, κ=0.41. The Von Karman Length Scale is representative of the length scale of the larger turbulent structures. It is compared to the RANS length scale $L=k1/2/(C\mu 1/4.\ \omega)$. If $L>L_{vk}$, meaning that the RANS length scale is larger than the length scale of the larger resolved eddies, the source term in the ω equations increases the production of ω, and so increases the dissipation of kinetic energy. This allows the development of smaller turbulent structures. In boundary-layer regions, L_{vk} reverts to the usual mixing-length formula and is given by:

$$L_{vk} = \kappa \frac{\partial \bar{u} / \partial y}{\partial^2 u / \partial y^2} \tag{7}$$

In other words, in boundary-layer regions the SAS model behaves as a RANS model, and in detached regions the SAS model works as a LES model, capturing the main complex 3D turbulent structures of the flow

3.3 Computational mesh and numerical solution

The size of the computational domain was defined in such a way that the boundaries do not interfere in the detached wake of the obstacle. A far field considering a width of twelve (12) obstacle diameters (*d*), a height of three times the height of the obstacle, i.e. 12*d*, and a length of 36.2*d* as commented in section 2. At the sides and ceiling boundaries the usual free slip wall condition was imposed. A run considering opening boundaries at these locations is in progress but results are not shown in this paper. At the entrance a normal constant velocity equal to U_∞ was imposed and an averaged pressure free flow (i.e., all velocity derivatives equal to zero) at the outlet region. The LES/SAS full hexahedral mesh was built based on the boundary layer thickness. It was estimated and its value divided by 10 to determine the first cell size. Starting from the obstacle walls a growth factor of 1.05 was applied in all directions. The boundary layer estimation tickness for laminar flow for Re=11,000, resulted in $\delta \cong$ 6e-4 m and the first cell size, therefore, was taken as 6e-5 m. This value leads to a maximum $y^+ \sim 3$, which was considered acceptable. The mesh used for the LES and SAS turbulence models is shown in Figure 2. A local refinement using an O-grid was defined near the obstacle, avoiding the usual "reflection" of structured meshes, allowing to define a likely constant grid spacing in the detached flow region, as recommended in LES models.

For the case where the unsteady k-ω SST turbulence model has been used, the mesh is almost 4 times coarser, due to the fact that this model does not need to capture scales of the flow which are modeled in this formulation. The size of the mesh used in LES and SAS approaches was 7.5 million nodes and for the k-ω SST model about 2 million nodes.

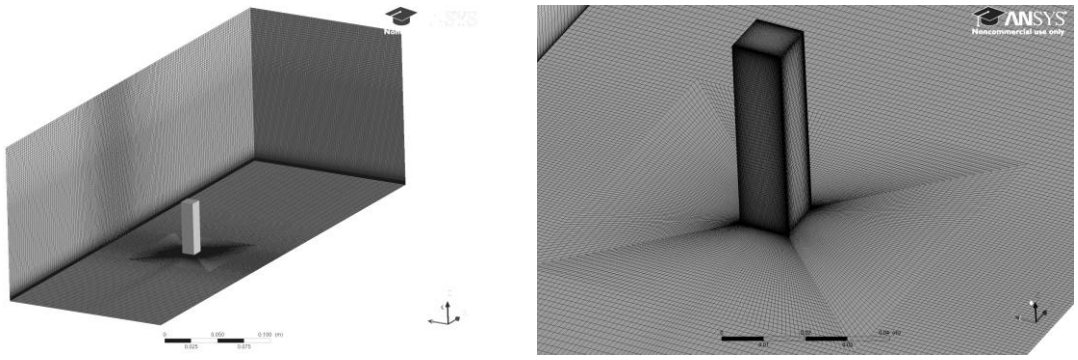

(a) (b)

Figure 2 - LES/SAS mesh overview(a). Zoom in the LES/SAS mesh around the obstacle (b)

Numerical computations were performed using the commercial package ANSYS CFX 13.0. This software is based on a discretization of the governing equations using and Element-based Finite Volume Method EbFVM ([14]) and a coupled approach for solving the pressure-velocity coupling ([15]). In all models, even for RANS approach (k-ω SST model) transient computations were developed, considering the same time step, which was set to Δt = 5e-6. This value led to a maximum Courant number of about 3, for LES Dynamic model. As the solution is fully implicit, only one iterative loop within each time step is needed to treat the non-linearity of convective terms in momentum equations. A maximum residual in momentum equation solver within each time step was set to 1e-3. A high resolution interpolation function ([16]) was used in k-ω SST and a Central Differencing Scheme (CDS) was used in LES simulations. For the SAS model a blending between both of them was used, where the high resolution scheme is used in the URANS region and CDS is used elsewhere.

4. RESULTS AND DISCUSSION

4.1 Averaged profiles

Velocity profiles have been time-averaged for all three models and compared with transient averaged experimental values provided by the challenge organization of the CFD Challenge 2012. The results were compared along lines transversal to the flow direction (contained in a horizontal (y-x) plane located at half the height of the obstacle, as shown in Figure 1.

Dimensionless average velocity profiles for U and V components obtained from the three models are shown in Figure 3.

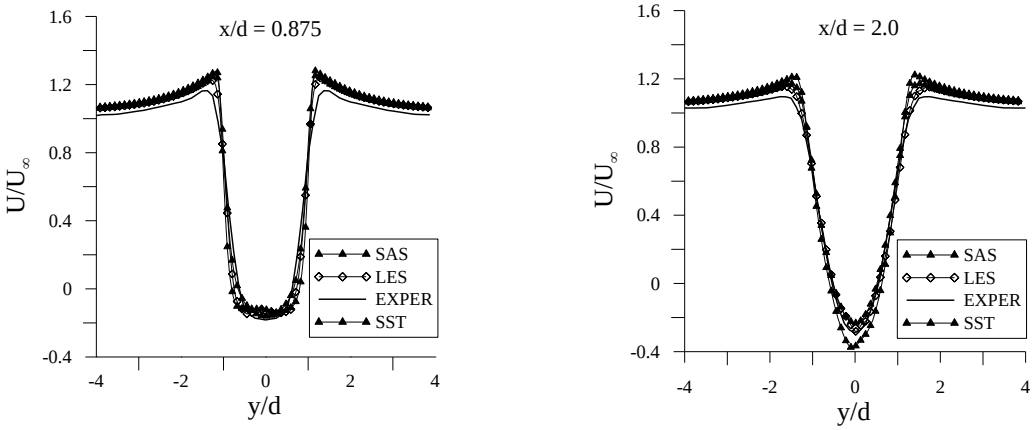

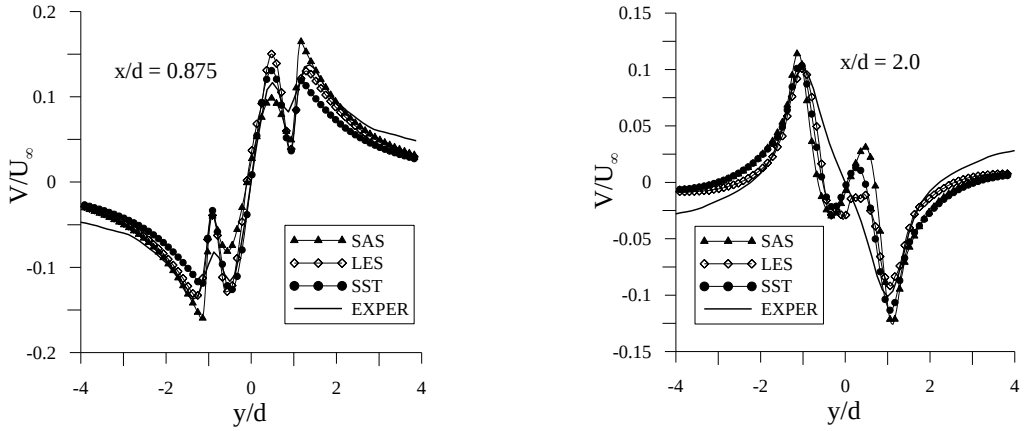

Figure 3 - Average velocity profiles, after the obstacle (along lines shown in Figure 1)

Velocity fluctuation correlations at the wake region are presented in Figure 4 for LES and SAS approaches, compared to experimental data. A zoom clipping the LES approach results is included in the ⟨u'v'⟩ profile for line x/d = 0.875 (i.e. very near downstream of the obstacle), in order to distinguish the SAS results. In this region, LES model seems to over-predict the experimental values for both u'_{RMS} and ⟨u'v'⟩. This could maybe due to the lack of an enough refined mesh in this region where turbulent scales are small and the relative mesh size to the turbulent scales does not satisfy the LES filtering criterion. On the other side, the SAS model is able to deal with this by resolving the scales not captured by the grid through RANS approach.

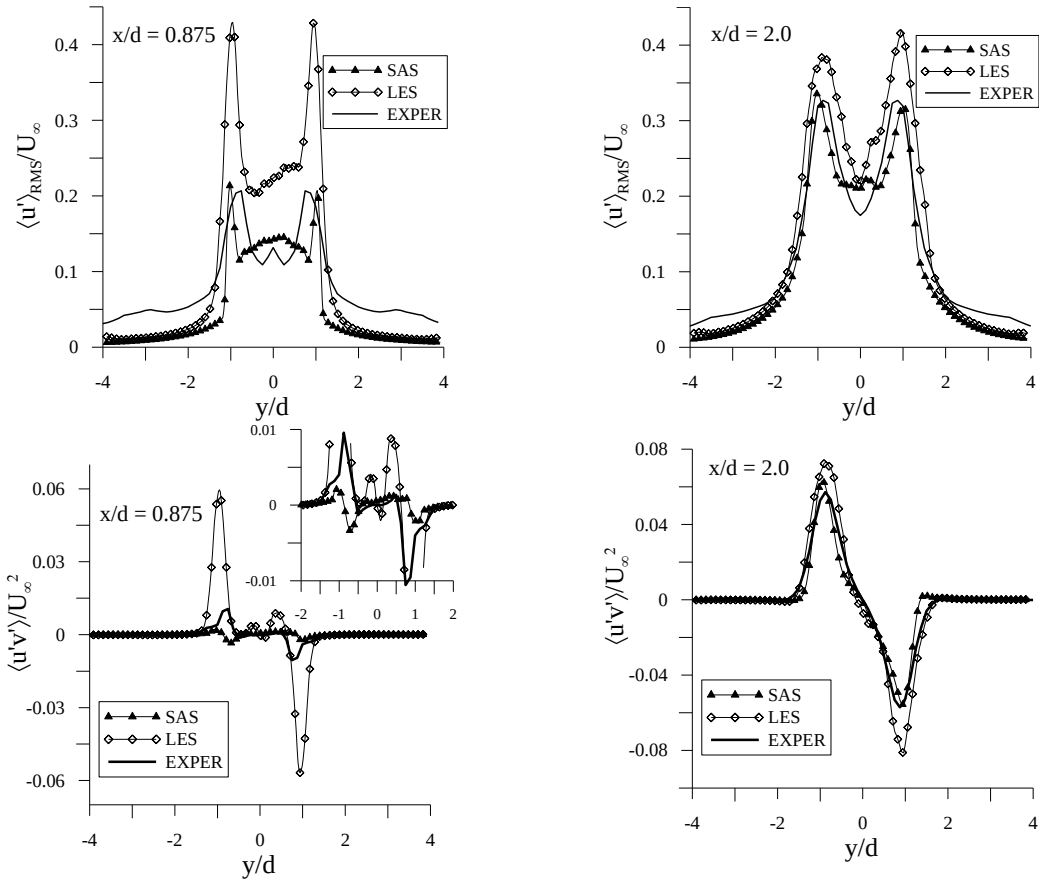

Figure 4 - Velocity fluctuation correlations (along lines shown in Figure 1)

Farther from the obstacle, both models adequately predict the velocity fluctuation correlations, though SAS results are closer to experimental values.

Another aspect which is currently under investigation is the validity of using free slip boundary conditions at the laterals and top of the domain for the dimensions used for the computational domain. As can be seen in Figure 3, there is a slight over-prediction of velocities close to where the free slip conditions was applied. These differences are more relevant as we go farther from the obstacle, as can be seen in Figure 5. This may indicate that the free slip walls were located too near the obstacle, even having 13*d* as size of the computational domain in the y-direction. There is a compromise here in terms of CPU cost; locate free slip (more stable) boundaries farther from the obstacle, which implies in a larger mesh if the grid size is maintained, or use an outlet condition which could introduce instabilities if vortices go through it. A run considering open boundaries at the laterals and top boundaries is ongoing, and results will be reported as soon as available.

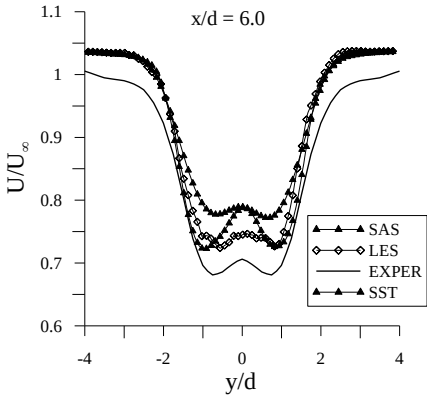

Figure 5 - Averaged U velocity profiles, in a line located at 6d downstream the obstacle

4.2 Tridimensional Flow Structure

Grayscale maps of instantaneous and averaged velocity in a plane z=2 are presented in Figure 6. As expected, while transient average velocity fields are similar for the three approaches considered in this paper. In all cases, the fields were averaged along a period of around 0,08 s for LES and SAS and 0,06 s for SST.

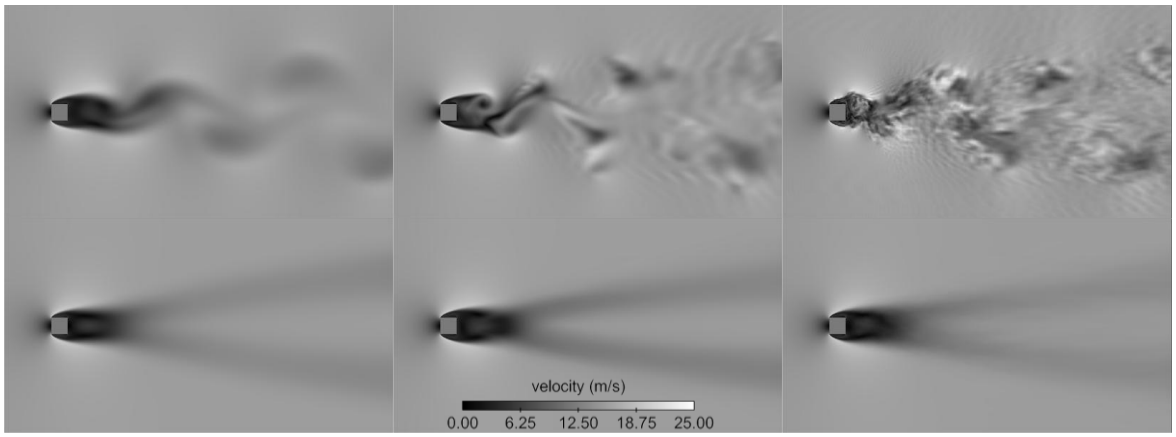

SST SAS LES

Figure 6 - Velocity map for SST, SAS and LES models. Instantaneous and averaged fields

The tridimensional wake structure can be seen in Figure 7, where iso-surfaces of λ_2 (see, for instance, [17]) calculated through the instantaneous and averaged velocity fields are shown for the SAS and LES models. The structures for the averaged flow are similar in both models, but some incoherent scales still appear in the LES case, indicating that a higher averaging time should be used.

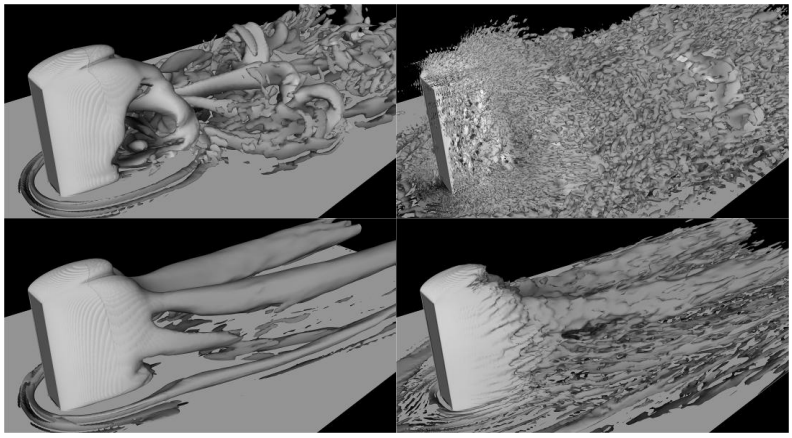

SAS LES

Figure 7 - Velocity map for SAS and LES models. Instantaneous and average fields

5. FINAL REMARKS

Three turbulence approaches had their results compared to experimental data measurements for a flow around a square cylinder. The RANS model, k-ω SST, presented good results when average quantities are compared. However, as expected, this turbulence model is not able to capture some important contribution of turbulent structures. On the other hand, the LES model presented good comparisons with the measured results in terms of average quantities, but over-predicts the results for Reynolds stresses components near the body. The SAS turbulence model has shown very good results and seems to be adequate to be used in some industrial applications. Approximate CPU time for SST, SAS and LES, when normalized, were, respectively, 1.0, 2.78 and 2,91. Although the SAS model CPU requirements are of the same order of LES, this is because the same time step was used for all models, for the sake of comparisons. Nonetheless, higher time steps than used here, like Δt=5e-6 s for example, led to divergence in LES simulations. Admissible time steps for SAS model were higher than these values and, in addition, less refined grid would be necessary near the walls. Thus, in an industrial problem, total CPU requirement in SAS model should certainly be much lower than LES approach.

REFERENCES

[1] CFD Society of Canada, CFDSC 2012 Challenge, http://www.cfdcanada.ca/challenge, 2012.
[2] Lilly, D. K., , Physics of Fluids A, Vol. 4, pp 633-635, 1992.
[3] Craft, T.J., "Non-Linear Eddy-Viscosity Models.", Lecture Notes, Department of Mechanical, Aerospace & Manufacturing Engineering, UMIST, 2012.
[4] Germano, M.; Piomelli, U.; Moin, P.; Cabot, W.H., Dynamic Subgrid-Scale Eddy Viscosity Model, Summer Workshop, Center for Turbulence Research, Stanford, 1996.
[5] Lardeau, S.;Leschziner, M.A. Computers&Fluids 34, pp. 3-21, 2005.
[6] Layton, W.J., A mathematical introduction to Large Eddy Simulation, Technical Report, Department of Mathematics, University of Pittsburgh, 2002.
[7] Pope, S.B., Turbulent Flows, Cambridge University Press, 1st Edition, 2000.
[8] Rodi,W., Journal of Wind Engineering and Industrial Aerodynamics 46&47, pp. 3-19, 1993.
[9] Shur, M.L.; Spalart, P.R.; Squires, K.D.; Strelets, M.; Travin, A., AIAA Journal 43, pp. 1230-1242, 2005.
[10] Smagorinsky, J., Monthly Weather Review v. 91, n. 3, pp. 99-164, 1963.
[11] Spalart, P.R., Annual Review of Fluid Mechanics 41, pp. 181-202, 2009.
[12] Menter, F. R., AIAA Journal, 32, 1598-1605, 1994
[13] Menter, F. R. & Egorov, Y.. A Scale Adaptive Simulation Model Using Two-Equation Models, AIAA Paper 2005-1095, 2005.
[14] Baliga, B. R. and Patankar, S. V., Numerical Heat Tranfer, 3, 393-409, 1980.
[15] Raw, M. J., A New Control-Volume-Based Finite Element Procedure for Numerical Solution of the Fluid Flow and Scalar Transport Equations , University of Waterloo, Canada (1985).
[16] Barth, T. J., Jespersen, D. C., AIAA Paper (1989) Volume: 89-0366, Issue: 89-0366, Pages: 1–12
[17] Chakraborty, p.; Balachandar, S.; Adrian, R. J., Journal of Fluid Mechanics, 535, (2005) 189-214.